Transient regime duration in continuous-time neural networks with delay

K. Pakdaman,[1] C. Grotta-Ragazzo,[2] and C. P. Malta[3]
[1]*Department of Biophysical Engineering, Faculty of Engineering Science, Osaka University, Toyonaka 560-8531, Osaka, Japan*
[2]*Instituto de Matemática e Estatística, Universidade de São Paulo, Caixa Postal 66281, 05315-970 São Paulo, Brazil*
[3]*Instituto de Física, Universidade de São Paulo, Caixa Postal 66318, 05315-970 São Paulo, Brazil*
(Received 2 March 1998)

Finite transmission times between neurons, referred to as delays, appear in hardware implementation of neural networks and may interfere with information processing by inducing oscillations. In some networks these oscillations are transients. In this work, we examine these in a two-neuron network, and we show analytically that the duration of such transients increases exponentially with the delay.
[S1063-651X(98)07009-3]

PACS number(s): 87.10.+e, 07.05.Mh

Hopfield [1] showed that networks of graded-response continuous-time neurons (GRCTNs) could be used for tasks such as content addressable memories, in the same way as networks of two-state discrete-time units. One of the motivations behind his study was that the former can be easily implemented in hardware. His analysis relied on describing the dynamics of a network composed of GRCTNs by a system of differential equations admitting a Lyapunov function. This ensured that no matter how the network was initialized, it eventually stabilized in a steady state representing the retrieved information. Hopfield recognized that, in his formulation, he neglected the finite propagation velocities that appear in electrical circuits, and argued that as long as the resulting transmission delays remain small compared to other characteristic time scales of the network, the electrical circuit should behave as predicted by the theoretical model.

This claim has been the starting point of a number of studies [2] aiming to determine whether finite propagation times and the ensuing transmission delays do indeed affect the dynamics of graded-response neural networks defined by

$$\frac{dx_i}{dt}(t) = -\gamma_i x_i(t) + K_i + \sum_{j=1}^{N} W_{ij}\sigma_{ij}(x_j(t-A_{ij})), \quad (1)$$

where x_i is the activation of the ith neuron, and $1/\gamma_i$ its characteristic charge-discharge time, K_i is the input to the unit i, W_{ij} is the connection weight between units j and i, A_{ij} is the transmission delay between these two units, and σ_{ij} are sigmoidal functions.

The aforementioned studies mainly focus on the asymptotic dynamics of the system with delay. Some derive sufficient conditions to avoid delay-induced oscillations in otherwise convergent networks, in other words, they provide constraints on parameter ranges, such as connection weights, neuron gains, and delays that ensure that the system with delay has the same stable equilibria as the one without delay, and that most solutions eventually stabilize at these equilibria.

Numerical investigations indicate that even when precautions are taken to avoid delay-induced instabilities, oscillations may arise in the presence of delays. These are delay-induced transient oscillations (DITOs), and cannot be predicted by the analysis of the asymptotic dynamics of neural networks. Examples of DITOs were first reported in two mutually exciting neurons and in rings [3], but, to our knowledge, no analysis of this phenomenon has been carried out. In our previous work, we observed that when DITOs appear, the duration of the transients, that is, the time required for the system to stabilize at an equilibrium, increases as the characteristic charge-discharge time of the neurons tends to zero, or, equivalently, as the delay is increased [4]. In fact, DITOs can last so long that for practical purposes they are indistinguishable from sustained oscillations. Therefore, understanding the origin of DITOs in neural networks constitutes an important complement to the analysis of delay induced instabilities in order to avoid long lasting oscillations that deteriorate network performance.

We attributed the presence of DITOs to the fact that solutions of Eq. (1) transiently follow those of the difference system defined as

$$x_i(t) = \frac{1}{\gamma_i}\left[K_i + \sum_{j=1}^{N} W_{ij}\sigma_{ij}(x_j(t-A_{ij}))\right]. \quad (2)$$

System (2) can display attracting oscillations even when almost all solutions of the corresponding delay equation (1) are convergent. The fact that some solutions display transient oscillations before stabilizing at equilibrium is the result of the difference between the asymptotic dynamics of Eqs. (1) and (2).

We also computed the transient regime duration (TRD) and we observed that it increased exponentially with the delay. However, no detailed study of this phenomenon was carried out beyond the numerical evidence that we provided. The main purpose of this work is to confirm the numerical results through the analytical calculation of the TRD. To this end, we examine the dynamics of the following two-neuron network:

$$\begin{aligned} \frac{dx}{dt}(t) &= -x(t) + W\sigma_\infty(y(t-A)), \\ \frac{dy}{dt}(t) &= -y(t) + W\sigma_\infty(x(t-A)), \end{aligned} \quad (3)$$

where σ_∞ is the step function, i.e., $\sigma_\infty(x)=1$ if $x>0$, and -1 otherwise. We show that the dynamics of system (3) can be understood in terms of the iterations of a one-dimensional

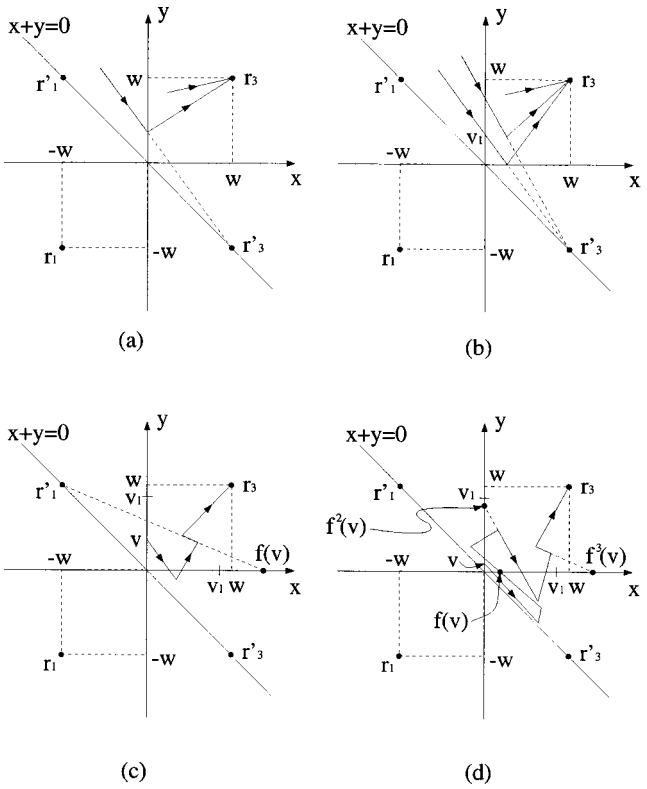

FIG. 1. Schematic construction of the map f. (a) for delay $A=0$, (b), (c), and (d) for delay $A>0$. See text for details.

map. We first provide a geometrical description of the construction of this map, and then we announce the general results.

Assuming that the delay A is set to zero, system (3) defines a two-dimensional ordinary differential equation, the trajectories of which in the (x,y) plane are easily constructed. We denote by $r_1=-(W,W)$, $r_2=(0,0)$, $r_3=(W,W)$, $r_1'=(-W,W)$, and $r_3'=(W,-W)$. r_1 and r_3 are the stable equilibria of the system to which most trajectories converge. Trajectories of initial conditions (u,v) with $u>0$ and $v>0$ are the segments of the straight lines connecting the initial point to r_3. An example of such a trajectory in the two-dimensional phase space is presented in Fig. 1(a). For an initial condition (u,v) with $0\leqslant -u<v$, the trajectory coincides first with the straight line connecting the initial point to r_3', until reaching the y axis, that is, as long as $x(t)<0$. From this point on, the trajectory is the segment connecting the intersection point with the y axis to the equilibrium point r_3. Thus, such trajectories are broken lines. One example is shown in Fig. 1(a). The trajectories of other initial conditions can be constructed in the same way.

In the following, we will mainly concentrate on the influence of delays on the trajectories of initial conditions satisfying either $u>0$ and $v>0$ or $0\leqslant -u<v$. These two regions of initial conditions are referred to as regions I and II, respectively. Trajectories of other initial conditions can be derived from these through symmetry considerations.

Since the input-output function of the neurons is a step function, delays do not alter the trajectories of initial conditions in I. These are the same as for the delay-less system, that is, segments connecting the initial condition to r_3, as exemplified in Fig. 1(b). The situation is different for initial conditions in II. In the case without delay, the effect of the sign change in x appeared instantaneously, as the trajectory switched to the straight line connecting r_3 right upon crossing the y axis. When interunit transmission is not instantaneous, this effect is delayed, that is, the trajectory continues along the same straight line towards the point r_3', during a time interval equal to the delay A, before switching to the segment that takes it towards the point r_3 [Fig. 1(b)]. For all trajectories starting in region II, the break points have exactly the same abscissae. Thus, there is a critical value of v, denoted v_1, such that the break point is exactly on the x axis [Fig. 1(b)]. This point plays an important role, as all initial conditions in II whose trajectories crosses the y axis above v_1 reach the stable point r_3 after exactly *one* break point, such as the one shown in the figure. Trajectories of other initial conditions will display two or more break points because they enter the region where $y<0$, that is, at some point, the second variable changes sign. This sign change will affect the trajectory after a time delay, and provoke a second break point, where the trajectory switches to the straight line leading towards r_1'. Other break points follow this, so that eventually the broken line representing the trajectory will end up at the equilibrium point r_3. An example of a trajectory with three break points is shown in Fig. 1(c).

Our analysis hinges upon the construction of a map that describes the trajectories after the second break point. Let us first note that the break points and the trajectories of initial conditions in II are entirely determined by the ordinate v at which the trajectory first intersects the y axis. So that in the following we only take this value into consideration. Then, for a given value v the construction of the map relies on the observation that we can find a point on the x axis, denoted $f(v)$ in Fig. 1(c), whose trajectory coincides exactly with that of the original initial condition *after* the second break point. Geometrically, this point is easily obtained as the intersection point between the x axis and the straight line connecting r_1' to the second break point of the trajectory. Thanks to this simple geometrical construction, we obtain $f(v)$ analytically as

$$f(v)=\frac{W(2+e^{-A})v}{2W-(v+W)e^{-A}}. \tag{4}$$

Once the point $(f(v),0)$ on the x axis is determined, we can reiterate the same analysis and construction assuming that the initial condition is in fact this new point. Thus, we can easily see that if $f(v)>v_1$, the trajectory will have only one more break point before tending to the equilibrium point r_3 along a straight line. This situation is represented in the Fig. 1(c). Conversely, when $f(v)<v_1$, the trajectory will have at least two more break points, since it will cross the y axis again. For such points, we can construct a point $(0,s)$ on the y axis such that the trajectory after the second break point, i.e., the fourth break point along the trajectory starting from the initial condition, coincides with that of $(0,s)$. Thanks to the symmetries of the system, we have $s=f(f(v))=f^2(v)$. If $f^2(v)>v_1$, we stop the process because after the fifth break point, the trajectory will converge to the stable equilibrium point along a straight line, otherwise, we continue to iterate f until there is n such that $f^n(v)>v_1$ [Fig. 1(d)]. Such a value of n exists because $f(v)>v$ for all $v>0$. Figure 2

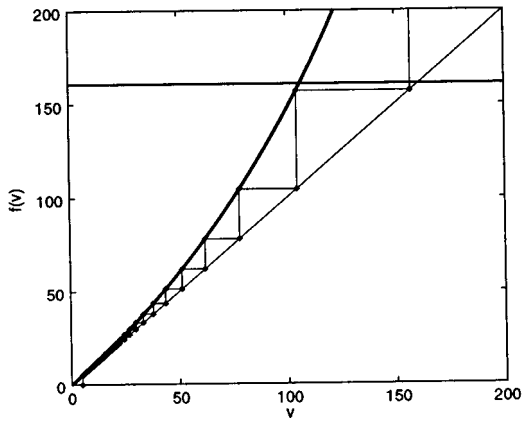

FIG. 2. Example of the map f. The solid line is the graph of the function f, the horizontal line is at v_1. The cobweb construction shows the successive iterates $f(V), f^2(V)=f(f(V)),\ldots,f^k(V)$ with $V=5$, until they become larger than v_1. Parameters: $W=3$, $A=4$. Abscissae and ordinates are in arbitrary units.

shows an example of the function f and the cobweb construction of the sequence of points $f^n(v)$, until it becomes larger than v_1.

We can formalize the above construction as follows:

Theorem. For $r=(u,v)\in\mathbb{R}^2$, such that $v>-u\geqslant 0$, let $V(r)=W(v+u)/(W-u)$ and n be the integer such that $f^{n-1}(V(r))<v_1\leqslant f^n(V(r))$, where $v_1=W(e^A-1)$. Then, there exist $T\geqslant nA$, and $\theta>0$ such that for $t\geqslant T$, $z(t,r)=z(t-\theta,r_n)$, where $z(t,\xi)$ is the solution of Eq. (3) through the initial condition ξ ($\xi=r$ or r_n), and r_n represents the point $[0,f^n(V(r))]$ on the y axis, for n even, and the point $[f^n(V(r)),0]$ on the x axis for n odd.

Our interest is in the transient oscillations of the solutions, and the incidence of these on the TRD, that is, the time it takes the trajectory to reach a small neighborhood of the equilibrium point. Using f and its iterates we can characterize both aspects of the dynamics of the system.

Oscillations for a system like Eq. (3) can be defined as points where either one of the variables x or y take the value zero, in other words, a solution oscillates as long as there are times t such that $x(t)\times y(t)=0$. We refer to such points as the zeros of the solution, and we denote by $N(r,A)$ the number of zeros of the solution of Eq. (3), with delay A, going through the initial condition r. The larger the value of N, and the more the solution oscillates. The following result shows that solutions of initial conditions $r=(u,v)$ in region II close to the straight line $u+v=0$ can display arbitrarily large numbers of zeros:

Transient oscillations. Let $v_n=f^{-n}(v_1)$, then

$$v_n=\frac{2W(2-e^{-A})^n(e^A-1)}{2(2+e^{-A})^n+[(2+e^{-A})^n-(2-e^{-A})^n](e^A-1)}.$$

We have $v_1(A)>v_2(A)>\cdots>v_k(A)>\cdots>0$, and v_n tends to zero as $n\to\infty$.

For $r=(u,v)\in\mathbb{R}^2$, with $0\leqslant -u<v$, we have $N(r,A)=1,2p$ and $2p+1$ $(p\geqslant 1)$ for $v>v_1-(1+v_1/W)u$, $v=v_p-(1+v_p/W)u$ and $v_{p+1}-[1+(v_{p+1})/W]u<v<v_p-(1+v_p/W)u$, respectively.

The number of zeros of a solution informs us about the TRD, because successive zeros cannot be arbitrarily close to one another, and as long as the solution is oscillating, it is obviously not stabilizing at the equilibrium point. Thus, any measure of the length of transient oscillations provides a lower bound for the TRD. We have the following result:

Transient regime duration. We denote by $T(r,A)$ the transient regime duration of a solution of Eq. (3), with delay A, going through the initial condition $r=(u,v)\in\mathbb{R}^2$, with $0\leqslant -u<v$. Then, $T(r,A)\geqslant pA$ for $v_{p+1}-[1+(v_{p+1})/W]u<v\leqslant v_p-(1+v_p/W)u$.

This result indicates that for fixed delay A, the TRD grows indefinitely as initial conditions get closer to the line $u+v=0$. Figure 3(a) shows the TRD as a function of the ordinate v for initial conditions $(-10^{-3},v)$. The TRD increases abruptly as v approaches 10^{-3}. The inset shows a magnification for v ranging from 20 to 50. The humps in the inset correspond to the changes in the number of zeros of solutions.

All the previous analyses were carried out for a system with fixed delay values. Our main concern is to see how the results are modified when the delay is increased. This is done in the following. The main result stems from the fact that the values $v_n(A)$ of the bounds delimiting the regions with a given number of zeros, and hence with a given range of TRD, increase exponentially with the delay.

Transient oscillations with the delay. For a fixed initial condition $r=(u,v)$ with $0\leqslant -u<v$, there is a strictly increasing sequence $0<A_1<A_2<\cdots<A_k<\cdots$, such that $z(t,r)$, the solution of Eq. (3), with delay A, going through r, displays exactly 1, $2p$, or $2p+1$ zero(s) for $A<A_1$, $A=A_p$, or $A_p<A<A_{p+1}$, respectively. In other words: $N(r,A)=1$, $2p$, and $2p+1$ for $A<A_1$, $A=A_p$, and $A_p<A<A_{p+1}$, respectively.

Thus, for fixed r, $N(r,A)$ and consequently $T(r,A)$ are increasing functions of A, when A is large enough. The speed with which these quantities increase can then be determined by remarking that $v_n(A)\sim 2We^A/(n+2)$ as $A\to\infty$, and using the lower bound on the TRD provided above.

Exponential increase of transient regime duration. Let $r=(u,v)\in\mathbb{R}^2$, with $0\leqslant -u<v$, and let $p=[2We^A/(W+V)]-1$ where the brackets indicate the integer part, and $V=W(u+v)/(W-u)$. Then, we have $T(r,A)\geqslant pA$, as $A\to\infty$, or $T(r,A)\geqslant 2WAe^A/(W+V)$.

The thick solid line in Fig. 3(b) shows the delay A versus the TRD plotted in a logarithmic scale for a fixed initial condition $r=(-10^{-3},5)$. It can be seen that as the delay is increased, the TRD increases linearly with the delay A, confirming our analytical results. This is in good agreement with the thin solid line, which shows the analytical lower bound for the TRD.

All the analysis and results presented until this point were carried out for a steplike input-output function σ_∞. This assumption allowed us to carry a detailed analytical description of the system dynamics. Numerical investigations show that similar results hold for the system

$$\begin{aligned}\frac{dx}{dt}(t)&=-x(t)+W\sigma_\alpha(y(t-A)),\\ \frac{dy}{dt}(t)&=-y(t)+W\sigma_\alpha(x(t-A)),\end{aligned}\tag{5}$$

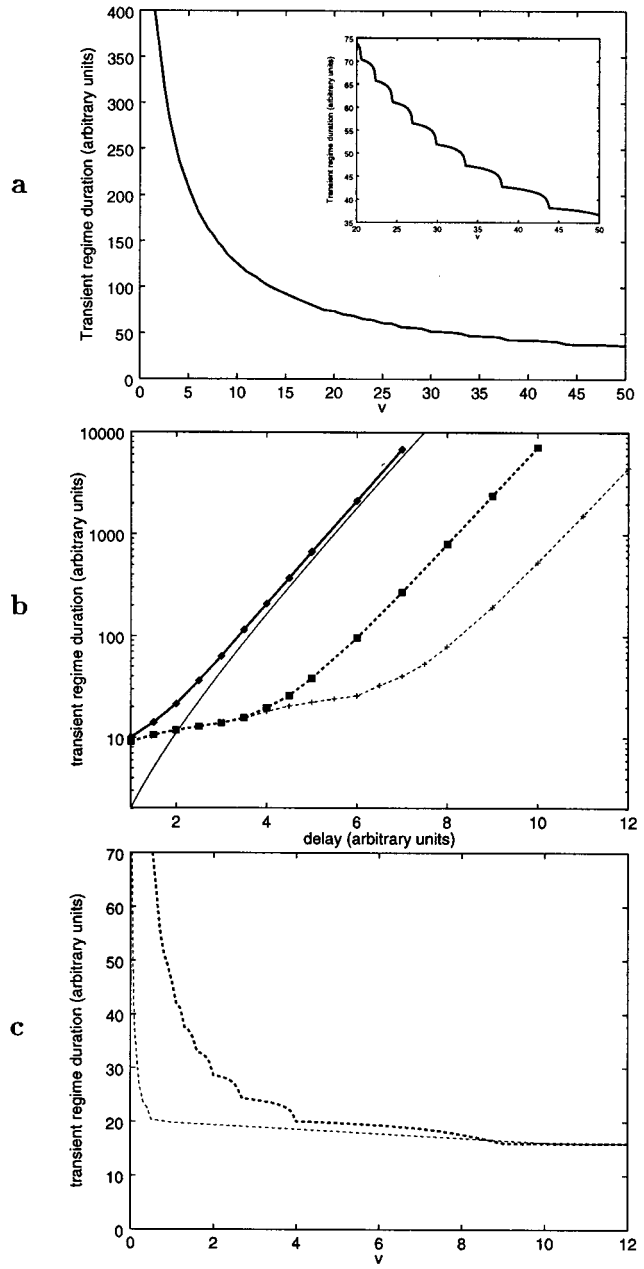

FIG. 3. Transient regime duration. (a) Transient regime duration for a delay $A=4$ for initial conditions (u,v) with $u=-10^{-3}$, and v ranging from 0.5 to 50. The inset shows a magnification of the graph for v in [20,50]. Abscissae: ordinate v of the initial condition, in arbitrary units; ordinates: transient regime duration in arbitrary units. (b) Delay vs the transient regime duration for the initial condition $(u,v)=(-10^{-3},5)$, for stepwise (thick solid line) and two smooth input-output functions with gain $\alpha=50$ (thick dashed line) and $\alpha=10$ (thin dashed line). The thin solid line is the analytical lower bound (see text for details). Abscissae: delay in arbitrary units; ordinates: transient regime duration in logarithmic scale, in arbitrary units. (c) Same as in A for smooth input-output functions with gains $\alpha=50$ (thick dashed line) and $\alpha=10$ (thin dashed line). Weight $W=3$ in all figures.

where the input-output functions of the units are smooth functions $\sigma_\alpha(x)=\tanh(\alpha x)$. The asymptotic dynamics of Eq. (5) has been described in [5]. In the following, we remind the results essential for our study.

Theorem. (i) When $0<\alpha W\leqslant 1$, the origin is a globally asymptotically stable equilibrium point of system (5).

(ii a) When $\alpha W>1$, system (5) has three equilibrium points denoted $r_1=(-a,-a)$, $r_2=(0,0)$, and $r_3=(a,a)$, where a is the unique strictly positive real number satisfying $a=W\sigma_\alpha(a)$. The points r_1 and r_3 are locally asymptotically stable, while r_2 is unstable.

(ii b) The union of the basins of attraction of r_1 and r_3 contains an open dense subset of the phase space.

(ii c) The complement of the union of the basins of attraction of the two stable equilibria, denoted $\mathcal{B}$, is the boundary separating the two basins.

(ii d) $\mathcal{B}$ is a codimension-one locally Lipschitz manifold containing the unstable equilibrium point $r_2=0$ and its stable manifold. It divides the phase space into two regions in the same way a plane divides a three-dimensional space: Points ''below'' and ''above'' $\mathcal{B}$ form the basins of attraction of r_1 and r_3, respectively.

The above result shows that no matter what value the delay A takes, most solutions of Eq. (5) tend to an equilibrium point. Those that are not convergent can only be contained in the narrow region forming the boundary separating the basins of attraction of the two stable equilibria when $\alpha W>1$. Therefore, the presence of delays does not alter the asymptotic dynamics of most trajectories of Eq. (5). However, for $\alpha W>1$, due to the presence of attracting periodic solutions of the difference system associated with Eq. (5), transient oscillations appear. The increases in the TRD due to the onset of these transient oscillations can be seen in Fig 3(c), for a fixed delay value, as the initial condition is changed, and the two dashed lines in Fig. 3(b) for a fixed initial condition, as the delay is changed. The results are similar to the case with the steplike input-output function. They also show that the TRD increases more rapidly for large α, the fastest increase being the one computed for the step input output function.

One key aspect in our analysis was the description of the dynamics of the two-neuron network with piecewise constant input-output functions and delayed interactions by the iterations of simple one-dimensional maps. Similar maps, albeit of appropriate dimension, can be constructed for networks composed of N units.

Assumptions for the existence of transient oscillations are that (i) the network with delay is almost convergent for all delays, and (ii) the associated discrete time network displays an attracting periodic orbit. Let us denote by $p_1,\ldots,p_k$ the successive points of this periodic orbit. Each p_i belongs to a given orthant, denoted by O_i, of the N-dimensional space. Transient oscillations arise when trajectories of the continuous-time system with delay follow for some time this periodic orbit, and the construction of the map is based upon this property. This construction is schematically described in the following.

Trajectories starting in O_i are segments of straight lines that connect the initial conditions to p_{i+1} (where $p_{k+1}=p_1$). These trajectories leave O_i through part of its boundary that we denote by B_i. For example, for the two-neuron network we studied, there is a period-two orbit, with $p_1=(-W,W)$ and $p_2=(W,-W)$. The corresponding orthants and boundaries are, respectively, $O_1=\{(u,v):u<0,v>0\}$, $O_2=\{(u,v):u>0,v<0\}$, and $B_1=\{(0,v):v>0\}\cup\{(u,0):u<0\}$, $B_2=\{(0,v):v<0\}\cup\{(u,0):u>0\}$. Each B_i can be

partitioned into two subsets, denoted by C_i and D_i, where trajectories starting in C_i enter O_{i+1} while those starting in D_i do not. In the case of the two-neuron network, we have $C_1=\{(0,v):0<v<v_1\}\cup\{(u,0):-v_1<u<0\}$ and $D_1=B_1-C_1$, while C_2 and D_2 are defined in a similar way. We can construct a map f_i that associates a point z' in B_{i+1} to a point z in C_i, such that the trajectories of the two points coincide after some appropriate time. This $(N-1)$-dimensional map generalizes the one used for the analysis of the two-neuron network. Its construction follows the same line.

Trajectories starting in C_i enter O_{i+1} after possibly going through a number of other orthants. These translate into a number of break points along the trajectory, before it joins a straight line leading to p_{i+2} ($i+2$ taken modulo k). The point $z'=f_i(z)$ is the intersection between this line and the boundary B_{i+1}. If z' is in C_{i+1}, the process can be continued to obtain a point z'' in B_{i+2}, otherwise, it stops. Therefore, in principle, it is possible to analyze the transient dynamics of an N-neuron network with delay through the composition of appropriate $(N-1)$-dimensional maps f_i, in the same way as for the two-neuron network.

The above construction generalizes the one in [6], introduced for the study of some oscillating solutions of networks composed of units with piecewise constant input-output functions with instantaneous transmission times [7,8]. It can be shown that the hypotheses in [6] imply the existence of an attracting periodic orbit $p_1,\ldots,p_k$ for the associated discrete-time neural network, so that the corresponding Poincaré map is one special form of the map depicted in the previous paragraph. However, important conditions for the application of the results in [6] are that (i) the orthants O_i and O_{i+1} be adjacent, (ii) trajectories initiated in the boundaries separating O_i from any neighboring orthant, except for O_{i+1}, enter O_i. This simplifies the construction of the map, even when interactions are delayed. Indeed, in this case, intermediate break points do not occur along trajectories, nor do orthant boundaries need to be subdivided. Furthermore, as we have shown through the study of a two-neuron network with delayed negative feedback [9] satisfying the above conditions [7], they imply that, regardless of the fact that the network without delay is convergent or not, the introduction of delays leads to *sustained* stable oscillations in such networks. Thus, they are subject to delay-induced loss of stability and do not satisfy our first assumption for the existence of delay-induced transient oscillations, namely, that delays be harmless for the asymptotic dynamics.

In conclusion, through our analytical study we have confirmed the fact that, due to the presence of DITOs, the transient regime duration of neural networks increases exponentially with the delay, even when the delay does not affect the asymptotic behavior of most trajectories. The DITOs are due to the fact that the solutions of Eq. (1) are transiently attracted by oscillating solutions of the associated difference system (2). Thus, even though the asymptotic dynamics of a network of GRCTNs is not affected by the delay, its information retrieval performance may deteriorate due to the DITOs that can cause a considerable lengthening of the transient regime duration.

The authors were partially supported by USP–COFECUB under Project No. U/C 9/94. C.P.M. and C.G.R. were also partially supported by CNPq (the Brazilian Research Council).

[1] J. J. Hopfield, Proc. Natl. Acad. Sci. USA **81**, 3088 (1984).

[2] J. Bélair, J. Dyn. Diff. Equ. **5**, 607 (1993); V. L. Kharitonov and A. D. B. Paice, *ibid.* **9**, 67 (1997); J. Bélair, S. A. Campbell, and P. van den Driessche, SIAM (Soc. Ind. Appl. Math.) J. Appl. Math. **56**, 245 (1996); J. Bélair, and S. Dufour, Canad. Appl. Math. Quarter. **4**, 136 (1996); T. A. Burton, J. Appl. Math. Stochast. Anal. **4**, 313 (1991); T. A. Burton, Neural Networks **6**, 677 (1993); Y. J. Cao and Q. H. Wu, IEEE Trans. Neural Netw. **7**, 1533 (1996); H. Chunhai and Q. Jixin, *ibid.* **9**, 221 (1998); K. Gopalsamy and X.-Z. He, *ibid.* **5**, 998 (1994); K. Gopalsamy and I. K. C. Leung, *ibid.* **8**, 341 (1997); K. Pakdaman and C. P. Malta, *ibid.* **9**, 231 (1998); P. P. Civalleri, M. Gilli, and L. Pandolfi, IEEE Trans. Circuits Syst., I: Fundam. Theory Appl. **40**, 157 (1993); M. Gilli, *ibid.* **40**, 849 (1993); M. Gilli, *ibid.* **41**, 518 (1994); T. Roska, C. W. Wu, M. Balsi, and L. O. Chua, *ibid.* **39**, 487 (1992); T. Roska, C. F. Wu, L. O. Chua, *ibid.* **40**, 270 (1993); H. Ye, A. N. Michel, and K. Wang, *ibid.* **43**, 532 (1996); S. Arik and V. Tavsanoglu, *ibid.* **45**, 168 (1998); M. Finnochiaro and R. Perfetti, Electron. Lett. **31**, 2024 (1995); K. Gopalsamy and X.-Z. He, Physica D **76**, 344 (1994); K. Gopalsamy and I. Leung, *ibid.* **98**, 395 (1996); C. M. Marcus, F. R. Waugh, and R. M. Westervelt, *ibid.* **51**, 234 (1991); L. Olien and J. Bélair, *ibid.* **102**, 349 (1997); R. D. Hangartner and P. Cull, Biol. Cybern. **73**, 177 (1995); X. B. Liang and T. Yamaguchi, IEICE Trans. Fundam. Electron. Commun. Comput. Sci. **E80A**, 247 (1997); C. M. Marcus and R. M. Westervelt, Phys. Rev. A **39**, 347 (1989); V. Menon, Int. J. Neural Syst. **6**, 3 (1995); K. Pakdaman, C. P. Malta, C. Grotta-Ragazzo, and J.-F. Vibert (unpublished); T. Roska and L. O. Chua, Int. J. Circuit Theory Appl. **20**, 469 (1992); H. Ye, A. N. Michel, and K. Wang, Phys. Rev. E **50**, 4206 (1994); H. Ye, A. N. Michel, and K. Wang, *ibid.* **51**, 2611 (1995); Z. Yi, Int. J. Syst. Sci. **27**, 227 (1996); Z. Yi, S. M. Zhong, and Z. L. Li, *ibid.* **27**, 895 (1996).

[3] K. L. Babcock, and R. M. Westervelt, Physica D **28**, 305 (1987); P. Baldi and A. F. Attyia, IEEE Trans. Neural Netw. **5**, 612 (1994).

[4] K. Pakdaman, C. P. Malta, C. Grotta-Ragazzo, and J.-F. Vibert, Neural Comput. **9**, 319 (1997); K. Pakdaman, C. P. Malta, C. Grotta-Ragazzo, O. Arino, and J.-F. Vibert, Phys. Rev. E **55**, 3234 (1997).

[5] K. Pakdaman, C. Grotta-Ragazzo, C. P. Malta, and J.-F. Vibert, Neural Networks **11**, 509 (1998).

[6] L. Glass, and J. S. Pasternak, J. Math. Biol. **6**, 207 (1978).

[7] J. E. Lewis and L. Glass, Neural Comput. **4**, 621 (1992).

[8] T. Mestl, C. Lemay, and L. Glass, Physica D **98**, 33 (1996).

[9] K. Pakdaman, C. P. Malta, C. Grotta-Ragazzo, P.-Y. Boelle, and J.-F. Vibert (unpublished).